HHS Public Access

Author manuscript

Ann Biomed Eng. Author manuscript; available in PMC 2017 December 01.

Published in final edited form as:

Ann Biomed Eng. 2016 December ; 44(12): 3510–3521. doi:10.1007/s10439-016-1683-6.

Imaging Spatiotemporal Activities of ZAP-70 in Live T Cells Using a FRET-based Biosensor

Kaitao Li[1,ŧ], **Xue Xiang**[1,2,†,ŧ], **Jie Sun**[3,‡], **Hai-tao He**[4], **Jianhua Wu**[2,§], **Yingxiao Wang**[3,*], and **Cheng Zhu**[1,¶]

[1]Coulter Department of Biomedical Engineering, Georgia Institute of Technology, Atlanta, Georgia, United States

[2]School of Life Sciences, SUN YAT-SEN University, Guangzhou, China

[3]Department of Bioengineering and Beckman Institute for Advanced Science and Technology, University of Illinois, Urbana-Champaign, Urbana, Illinois, United States

[4]Centre d'Immunologie de Marseille-Luminy, Aix Marseille Université UM2, Inserm, U1104, CNRS UMR7280, 13288 Marseille, France

Abstract

The zeta-chain-associated protein kinase 70 kDa (ZAP-70), a member of the spleen tyrosine kinase (Syk) family, plays an essential role in early T cell receptor (TCR) signaling. Defects in ZAP-70 lead to impaired thymocyte development and peripheral T cell activation. To better understand its activation dynamics and regulation, we visualized ZAP-70 activities in single live T cells with a Förster resonance energy transfer (FRET)-based biosensor, which was designed for probing kinase activities of the Syk family. We observed in Jurkat E6.1 T cells rapid and specific FRET changes following anti-CD3 stimulation and subsequent piceatannol inhibition. The initiation of ZAP-70 activation was prompt (within 10 sec) and correlates with the accompanied intracellular calcium elevation, as revealed by simultaneous imaging of the biosensor and calcium. Different from the previously reported ZAP-70 activation in the immunological synapse and the opposite pole (anti-synapse), we have observed rapid and sustained ZAP-70 activation only at the synapse with superantigen-pulsed Raji B cells. Furthermore, ZAP-70 signaling was impaired by cholesterol depletion, further supporting the importance of membrane organization in TCR signaling. Together our results provide a direct characterization of the spatiotemporal features of ZAP-70 activity in real time at subcellular levels.

Key terms

TCR signaling; Syk family kinase; Immunological synapse; Membrane microdomains

¶To whom correspondence and reprint request should address.
†Present address: UnionPay Smart Co.,Ltd, Shanghai, China
‡Present address: Center for Cell Engineering, Memorial Sloan Kettering Cancer Center, New York, United States.
§Present address: School of Bioscience, South China University of Technology, Guangzhou, China
*Present address: Department of Bioengineering, University of California, San Diego
ŧCo-first author

Introduction

TCR signaling relies heavily on the activation of ZAP-70, a member of the Syk family of tyrosine kinases.[2,27] Engagement of the TCR with cognate peptide bound to the major histocompatibility complex (pMHC) results in phosphorylation of the immunoreceptor tyrosine-based activation motifs (ITAMs) in the associated CD3 subunits. The dually phosphorylated ITAMs serve as docking sites for the tandem SH2 domains of ZAP-70, facilitating its recruitment to the TCR-CD3 complex and activation by Src family kinases, such as lymphocyte-specific protein tyrosine kinase (Lck) and proto-oncogene tyrosine-protein kinase (Fyn). Activated ZAP-70 then phosphorylates the linker of T cell activation (LAT) and several other intermediate molecules in the proximal signaling complex, such as the SH2 domain-containing leukocyte protein family members SLP-76, VAV family members, and phospholipase Cγ (PLCγ), which further induce various downstream responses that lead to T cell activation.[20,39] Mice and humans with ZAP-70 defects exhibit impaired thymocyte development and peripheral T cell activation, and suffer from severe combined immunodeficiency.[37] The pivotal role of ZAP-70 calls for a better understanding of its kinase activity in normal and diseased conditions as well as the underlying regulatory mechanisms.

ZAP-70 activation is commonly reported by Western blot with antibodies targeting the phosphorylation of two tyrosine sites: pY493 in the activation loop of the kinase domain that is required for its full catalytic activity, and pY319 in interdomain B that stabilizes its active conformation and binds Lck, facilitating the phosphorylation of Y493.[2] Rapid phosphorylation of these two tyrosine residues upon TCR engagement is accompanied by ZAP-70 translocation from the cytoplasm to the plasma membrane, as shown by fluorescence imaging.[32,33] At even higher spatial resolution, phosphorylated ZAP-70 was observed to localize in microcluters (200–500 nm-diameter) containing TCR and SLP-76 formed at the periphery of immunological synapse.[41] However, it is unclear how ZAP-70 activity is dynamically regulated at subcellular level.

Genetically encoded biosensors based on Förster resonance energy transfer (FRET) technology is evolving as a new generation of live cell imaging approach to monitor the dynamic intracellular signaling cascades.[31,34,38] FRET biosensors for ZAP-70 were reported with its detection of ZAP-70 kinase activity at both the immunological synapse and the opposing pole of synapse.[8,29] Based on the same principle, we have developed and validated a biosensor specific for Syk family kinases and observed Syk activation through FcγRIIA and PDGF receptor signaling.[40] Since Syk and ZAP-70 are differentially expressed in immune cells (e.g. mature conventional T cells expressing only ZAP-70), we tested the feasibility of using the biosensor to report ZAP-70 activity in T cells. We expressed the biosensor in Jurkat T cells and observed rapid (within 10 sec upon TCR stimulation) FRET changes specific to ZAP-70 activation. Concurrent imaging of the biosensor and calcium reveals that ZAP-70 activation is correlated with the early calcium elevation. Stimulation of Jurkat E6.1 cells with superantigen-pulsed Raji B cells induced rapid and sustained ZAP-70 activation with a much higher ZAP-70 activities in immunological synapse than in anti-synapse or in cytosol. Furthermore, ZAP-70 activity was suppressed by cholesterol

depletion, suggesting a critical role of membrane organization in ZAP-70 activity regulation within the TCR signaling network.

Materials and Methods

Cell culture and transfection

Raji B cells, Jurkat cell clones E6.1 and P116 were purchased from American Type Culture Collection. P116 cells expressing ZAP-70 KA were a kind gift of Dr. Arthur Weiss (University of California, San Francisco). Jurkat cells were transfected with the biosensor following the standard procedure established by Amaxa nucleofector. Typically, 3×10^6 cells were transfected with 8 μg of plasmid DNA. 24 hours after transfection, cells were cultured in RPMI1640 supplemented with 10% fetal bovine serum (FBS), 100 U/ml Penicillin, 100 μg/ml Streptomycin and 2 mM L-glutamine in the presence of 1.2 mg/ml G418 as the selection regent. Stable cell lines were generated by FACS sorting of the CD3+YPet+ population.

Reagents

Anti-CD3 (clone OKT3), anti-ZAP-70 (clone 1E7.2), mouse IgG1 isotype control, and APC-conjugated anti-mouse IgG1 (clone M1-14D12) were from eBioscience. Rabbit anti-GFP (clone ab290) and goat anti-Rabbit IgG H&L (HRP) (clone ab6721) were from abcam. X-rhod-1-AM, probenecid, Dynabeads, and anti-β tublin antibody were from Invitrogen. Goat anti-mouse IgG peroxidase conjugated, and mouse anti-goat IgG H&L were from Thermo Scientifc. Rabbit anti-phosphoZAP-70 was from Cell Signaling. Mouse anti-phosphotyrosine 4G10 was from Millipore. Superantigen was a mix of recombinant staphylococcal enterotoxin E, staphylococcal enterotoxin A, staphylococcal enterotoxin B, and staphylococcal enterotoxin C3 coming from Toxin Technology. All chemicals and other reagents were from Sigma unless otherwise indicated.

In Vitro kinase assay

Biosensor was expressed with N-terminal 6× His-tag in *Escherichia coli* and purified by nickel chelation chromatography as previous described.[40] Fluorescence emission spectrum with 430 nm excitation of purified biosensor with a final concentration of 1 μM was measured in a 96-well plate using a fluorescence plate reader (TECAN, Sapphire II). Emission ratios of ECFP/FRET (478/526 nm) were measured in kinase buffer (50 mM Tris pH 8, 100 mM NaCl, 10 mM MgCl2, 2 mM dithiothreitol, 1 mM ATP) at 30°C before and after the addition of 1 μg/ml active ZAP-70 kinase (Calbiochem).

Immunoprecipitation and immunoblotting

3×10^7 Jurkat cells expressing biosensors were harvested, washed and resuspended in 200 μl HBSS working buffer, then stimulated or kept as a control before being lysing. For anti-CD3 stimulation, 10 μg/ml OKT3 was added to Jurkat cells suspension for 10 min at 37°C. For superantigen stimulation, 3×10^7 Raji B cells were pulsed with 200 ng/ml mixture of recombinant superantigen staphylococcal enterotoxin E, staphylococcal enterotoxin A, staphylococcal enterotoxin B, and staphylococcal enterotoxin C3 for 30 min at 37°C. Then biosensor-expressing Jurkat cells were mixed with superantigen-pulsed Raji B cells in a 1:1

ratio and spun down for incubation for the indicated time at 37°C. Reactions were ceased by adding cold HBSS working buffer into cell suspensions. After stimulation, cells were washed twice, and lysed with 300 μl ice-cold NP 40 lysis buffer (supplemented with 1mM PMSF, 1× protease inhibitor cocktail and 1× phosphatase inhibitor cocktail) for 30 min. Lysates were clarified by centrifuging at 14,000 g for 10 min at 4°C. Post nuclear supernatants were subjected to immunoprecipitation with an anti-GFP coated on Dynabeads Protein G. The cell lysates and eluted immunoprecipitants were separated by 10% SDS-polyacrylamide gel and analyzed by immunoblotting with indicated primary antibodies and corresponding secondary antibodies conjugated with peroxidase. Images were revealed by ECL.

Flow cytometry

Jurkat E6.1 and P116KA cells were fixed with cold 4% paraformaldehyde in PBS for 10 min at room temperature, washed and re-suspended in permeabilization buffer (HBSS, 0.1% saponin, 0.05% NaN_3), then stained for 1 hr with 10 μg/ml anti-ZAP-70 or mouse IgG1 isotype control followed by washing and staining with 10 μg/ml APC-conjugated anti-mouse IgG1 secondary antibody for an additional 30 min. The samples were processed using LSR flow cytometer (Becton Dickinson BD) and analyzed using FlowJo software (Stanford University-Tree Star).

Biosensor spectral imaging

1×10^6 Jurkat cells were harvested, washed twice and resuspended in 300 μl HBSS working buffer, or pretreated with 10 μM piceatannol for 30 min at room temperature. The Focht Chamber System 2 (FCS2; Bioptechs) was kept at 37°C and placed on the stage of a LSM 510 META Carl Zeiss laser scanning microscope (Jena, Germany). Cells were allowed to settle down on coverslips coated with Poly-L-Lysine and stimulated by injecting 10 μg/ml anti-CD3 or vehicle into chamber for 15 min and fixed. ECFP was excited at 840 nm (two-photon excitation) using a tunable Chameleon laser. Spectral images were acquired ranging from 440 nm to 580 nm. Emission intensity at individual wavelength was normalized to the average of intensities from all wavelengths. Data were collected from 3 experiments, each containing no less than 20 cells.

Immunostaining and imaging of pZAP-70

Jurkat E6.1 cells expressing biosensor were mixed with superantigen-pulsed Raji B cells in 1:1 ratio, then spun down and incubated for 2 min. Cells were fixed and permeabilized for intracellular staining with rabbit anti-pZAP-70, and then Cy5-conjugated goat anti-rabbit IgG. Images were acquired in a Zeiss LSM 510 NLO confocal microscope.

Epi-fluorescence imaging of ZAP-70 biosensor and calcium

Epi-fluorescence imaging of biosensor-expressing cells was performed using an Olympus IX70 inverted microscope equipped with a 60×, 1.45NA TIRF objective and the Micro-Manager 1.4 imaging software.[14] Jurkat cells expressing the biosensor were loaded into imaging chamber containing CO_2 independent medium with 5 mM HEPES and 1% BSA.

Cells were excited at 436/20 nm with the emissions of ECFP and YPet collected sequentially at 480/40 nm and 535/30 nm, respectively.

For simultaneous monitoring of calcium activity, Jurkat E6.1 cells expressing the biosensor were incubated with 5 μM X-Rhod-1-AM and 2.5 mM probenecid in PBS for 30 min and washed twice before imaging. Cells were excited alternately at 580/15 nm, 436/20 nm, 436/20 nm, and collected for X-Rhod-1, ECFP, and YPet emissions at 645/75 nm, 480/40 nm, and 535/30 nm, respectively.

Data analysis and statistics

All data were analyzed using customized Matlab (MathWorks) program and Excel (Microsoft). Raw image files were primed for analysis by subtracting background, denoising with a 3×3 median filter, and compensating for inter-channel cell motion. ECFP/FRET ratio is calculated as the ratio between emission channels of donor ECFP (480/40 nm, ECFP) and acceptor YPet (535/30nm, FRET) under the same donor excitation (436/20 nm). Ratio images were presented using IMD display mode.[35] Ratios were averaged across each cell as defined by binary mask of the FRET channel. Student t-test was performed for comparison between two groups. *, $p<0.05$; **, $p<0.01$; ***, $p<0.001$.

Results

Biosensor design and *in vitro* validation

We have previously developed the FRET biosensor for Syk family kinases and observed Syk activation upon FcγRIIA or PDGF receptor stimulation in K562 or MEF cells, respectively.[40] The biosensor consists of an ECFP-YPet FRET pair, a SH2 domain, a flexible linker, and a peptide sequence from Vav2, one of the substrates of Syk and ZAP-70 (Fig. 1a).[40] The biosensor works in the high FRET mode at rest state and switches to the low FRET mode when the substrate gets phosphorylated, which allows the intramolecular binding of the SH2 domain and subsequent separation of the FRET pair (Fig. 1b).[40] This FRET switch translates ZAP-70 kinase activities into changes in the ratio of ECFP (Donor) and YPet (Acceptor or FRET) emissions under the same donor excitation.

Knowing its high specificity to Syk, we then validated the biosensor using purified active ZAP-70 proteins (Fig. 1c). Addition of active ZAP-70 induced an increase in ECFP/FRET ratio on wild type (WT) biosensor over time that reached steady state level of 60% by 200 min, indicating ZAP-70-induced significant loss of FRET. Substitution of either kinase phosphorylation Tyr site with Phe (Y172F) in the substrate domain or Arg to Val (R175V) in the SH2 domain abolished the FRET response. This confirms that the biosensor alters FRET response to ZAP-70 in a phosphorylation-dependent manner as designed.

Biosensor responses are ZAP-70 specific in Jurkat T cells

To test the biosensor specificity in live cells, we expressed the biosensor in Jurkat E6.1 T cells, in which ZAP-70 is the only Syk family kinase expressed.[15] The emission spectral response was examined with stimulation of cells using anti-CD3 (Fig. 2a). Exciting ECFP alone resulted in a spectrum of unstimulated cells with a peak emission around 520 nm,

confirming the high FRET at the rest state. Stimulation with anti-CD3 enhanced ECFP emission (~476 nm) at the expense of YPet emission (~520 nm), which yielded 38% increase in the ECFP/FRET emission ratio (Fig. 2b). This spectral change was abolished in cells pretreated with piceatannol, an inhibitor for the Syk kinase family (Fig. 2a & b).[28]

To further confirm the biosensor specificity, we compared biosensor phosphorylation and FRET signals in WT (E6.1) versus ZAP-70-deficient (P116) Jurkat cells upon anti-CD3 stimulation. Cells were lysed and immunoprecipitated with anti-GFP antibody followed by immunoblotting with anti-pY antibody. Addition of soluble anti-CD3 triggered a significant increase of biosensor phosphorylation in E6.1 cells, as identified by the band at molecular weight of 70 kD; whereas no change was detected in P116 cells (Fig. 2c). Consistent with the phosphorylation events, E6.1 cells showed rapid and robust ECFP/FRET ratio increase (~20%) following anti-CD3 stimulation (Fig. 2d). By comparison, the P116 cells showed no detectable ECFP/FRET ratio changes, similar to the unstimulated control. These data indicate that biosensor phosphorylation and its FRET responses are ZAP-70 dependent in Jurkat T cells.

In addition to its kinase activity, ZAP-70 was also found to regulate TCR/BCR signaling and T/B cell functions through kinase-independent mechanisms.[3,9] To confirm that our biosensor reports the kinase activities of ZAP-70 instead of an indirect outcome of its kinase-independent regulation, we expressed the biosensor in P116 cells reconstituted with a kinase-inactive ZAP-70 mutant (ZAP-70 K369A).[6,9] Despite the ZAP-70 K369A expression in P116KA cells was similar to that of ZAP-70 in E6.1 cells (Fig. S1), P116KA cells failed to generate biosensor FRET response to anti-CD3 stimulation (Fig. 2d), further proving the faithful report of ZAP-70 kinase activities by this biosensor.

Biosensor reports ZAP-70 activities with fast kinetics in Jurkat T cells

To test the ability of our biosensor to report ZAP-70 activity with kinetics similar to endogenous signaling molecules, such as ZAP-70 and its substrates, we compared the phosphorylation kinetics of the biosensor in E6.1 cells with that of ZAP-70, SLP-76, and LAT following stimulation with superantigen-pulsed Raji B cells (Fig. 3a & b). Phosphorylation of ZAP-70 Y493 increased by 1 fold at as early as 2 min after stimulation, and peaked at 15 min in all the time points examined. In contrast, the maximum phosphorylation at ZAP-70 Y319 occurred much earlier (at 2 min), which is consistent with its role in binding Lck and facilitating the phosphorylation of Y493. Biosensor phosphorylation displays a 20% increase at 2 min, and peaked at 70% increase at 15 min, and then decrease to baseline at 30 min. This largely matches the kinetics of ZAP-70 pY493, which indicates its full activation. The phosphorylation kinetics of SLP-76 Y145 and LAT Y191 are slightly different with a peak at 2 min. This may be attributed to their location and dephosphorylation rates by phosphatases. Phosphorylated ZAP-70, SLP-76, and LAT are more concentrated near the membrane and are more easily to be dephosphorylated than the biosensor that diffuses freely in the whole cell, since phosphatases are also found to translocate to membrane upon TCR stimulation.[1]

We also evaluated the kinetics of biosensor FRET changes in response to positive and negative modulations of upstream signals by imaging individual E6.1 cells. Anti-CD3

induced ECFP/FRET ratio increase was observed at the first time point (30 sec) post stimulation and plateaued at ~20% increase within 90 sec (Fig. 3c), indicating rapid ZAP-70 activation. The high ECFP/FRET ratio then dropped to baseline within 1 min after addition of piceatannol (Fig. 3c), indicating a fast and specific reaction of the biosensor with ZAP-70. Moreover, the ratio went below baseline post piceatannol treatment, suggesting the inhibition of a basal ZAP-70 activity. Indeed, basal levels of phosphorylation of the biosensor, ZAP-70, SLP-76, and LAT were observed in E6.1 cells even without anti-CD3 stimulation (Figs. 2c & 3a). This basal activity was further revealed by inhibiting the upstream Src family kinases with PP2, which caused a 17% decrease of ECFP/FRET ratio in 5 min (Fig. 3d). On a single cell basis, the maximum percentage of ECFP/FRET ratio decrease is positively correlated with the ratio baseline (Fig. 3e), also suggesting that the biosensor reports the depletion of basal active ZAP-70 following PP2 treatment. Furthermore, the responses of the ZAP-70 biosensor to anti-CD3 and PP2 also match the activities of the upstream Src family kinases as measured using E6.1 cells expressing a Src biosensor (Fig. S2).[38]

Concurrent measurement of ZAP-70 activities and intracellular calcium

Numerous studies have demonstrated that stimulation of the TCR-CD3 complex induces a rapid increase of cytosolic [Ca^{2+}], released from intracellular Ca^{2+} stores via IP3 receptors.[21,36] As a kinase of early TCR signaling, ZAP-70 initiates several downstream signaling cascades, including PLCγ activation and subsequent IP3 production. To further explore the multiplexing capability of reporting hierarchical signaling events with the biosensor, we combined biosensor and calcium fluorescence imaging by loading calcium indicator X-rhod-1-AM into biosensor-expressing E6.1 cells. We observed the initiation of ZAP-70 activation within 10 sec upon addition of soluble anti-CD3, with a slight delay in calcium flux (Fig. 4a). At a 10-sec temporal resolution, rapid responses of the biosensor and cytosolic calcium were also observed in E6.1 cells stimulated with superantigen-pulsed Raji B cells (Fig. 4b). The increases of these two signals are much stronger and faster comparing with soluble anti-CD3 stimulation, and show positive correlation in the maximum magnitude within 2 min upon contact with B cells (Fig. 4c). The possible negative effect of DMSO in the calcium dye was excluded by comparing the ECFP emissions of biosensor-expressing cells with and without DMSO treatments (Fig. S3). These results indicate that ZAP-70 activation reported by the biosensor precedes or is accompanied by calcium release, further enhancing the role of ZAP-70 in early TCR signaling.

Biosensor reveals local ZAP-70 activation within the immunological synapse

A key process during T cell activation is the formation of immunological synapse with antigen-presenting cells.[7,16]. Immunological synapse provides a special interface, where the TCR, adhesion molecules and co-stimulatory receptors are redistributed, engaged, or internalized, triggering highly localized signaling cascades.[12,23,41] Intrigued by this local signal transduction, we sought to visualize the spatial and temporal pattern of ZAP-70 activity with the aid of our biosensor. The immunological synapse was observed within 2 min after E6.1 cells encountered superantigen-loaded Raji B cells and was accompanied by an immediate ZAP-70 activation mostly confined in the synapse (Fig. 5a & c). In contrast, P116 cells failed to generate significant FRET changes although nascent synaptic structures

were also observed (Fig. 5b & c). Interestingly, the kinetics of ZAP-70 activation is related to the 'quality' of synapses formed. Stable synapses lasting for more than 15 min generated much stronger and more sustainable ZAP-70 activation than unstable ones (Fig. 5c), suggesting distinct ZAP-70 signaling dynamics coupled with antigen recognition.

To further characterize the spatial pattern, we quantified ECFP/FRET ratio in three cellular compartments: the synapse, the anti-synapse (the distal pole of synapse[29]), and the cytosol. At both time points examined (2 min and 10 min after B cell encounter), no difference was found between anti-synapse and cytosol, whereas the ECFP/FRET ratio is significantly higher in synapse than in the other two compartments (Fig. 5d). The highly localized ZAP-70 activation is distinct from the more uniform pattern of ZAP-70 activity with soluble anti-CD3 stimulation (Fig. S4). Consistent with the biosensor-reported local signaling, fast and local phosphorylation of ZAP-70 in the immunological synapse was detected by anti-phospho-ZAP-70 immunostaining (Fig. S5).

Regulation of ZAP-70 activities downstream of TCR signaling depends on membrane organization

TCR signaling has been found to rely on the segregated membrane microdomains, where enriched cholesterol and sphingolipids are thought contributing to the spatial regulation of receptor triggering and signaling.[13,17] This is evidenced by the previous findings that some key molecules in TCR triggering are either associated with or recruited to the distinct membrane compartments upon TCR stimulation.[4,5,11,24] To examine how membrane organization impacts the dynamics of ZAP-70 activities, we imaged the biosensor responses of E6.1 cells treated with methyl-β-cyclodextrin (MβCD) that depletes cellular cholesterol. Comparing to non-treated cells, MβCD-treated cells exhibited much lower and transient ZAP-70 activation to anti-CD3 stimulation (Fig. 6a), as well as a much weaker deactivation to PP2 treatment, suggesting the importance of membrane organization in the proper regulation of ZAP-70 signaling.

Discussion

ZAP-70 activation is a crucial step in T cell activation upon TCR triggering, which amplifies the signal by phosphorylating various substrates, such as LAT, SLP-76, and the VAV family members. Defects in ZAP-70 could lead to impaired T cell development and effector functions.[37] Despite extensive studies of this molecule, it remains unclear how the kinase activity is dynamically regulated inside of live T cells. In this study, we characterized the specificity, kinetics, and spatial resolution of a FRET-based biosensor to ZAP-70 activity, and demonstrated its applications for direct visualization of the spatiotemporal distribution of ZAP-70 activities in individual Jurkat T cells. Using biosensor-expressing E6.1 cells, we observed ZAP-70-dependent rapid FRET loss upon anti-CD3 stimulation, which was promptly recovered by treatment of piceatannol, a ZAP-70 inhibitor. This fast and reversible FRET response is required for faithfully reporting ZAP-70 signaling dynamics. Our data was further strengthened by the similar phosphorylation kinetics comparing to endogenous ZAP-70 Y493 and by the concurrent increase in cytosolic calcium and the ECFP/FRET

ratio. The high specificity and fast kinetics of the biosensor response enabled us to evaluate both TCR-induced ZAP-70 activation and basal level of active ZAP-70 in resting cells.

To monitor the spatiotemporal patterns of ZAP-70 signaling, we used our biosensor to visualize the activation of ZAP-70 at a subcellular level. Stimulation of E6.1 cells with superantigen-pulsed Raji B cells induced ZAP-70 activation at local regions with a concomitant formation of immunological synapse. The ECFP/FRET ratio rapidly increased near the conjugating area from 1 min and sustained for 15 min, showing a distinct pattern of microdomain signal transduction. Considering the cytosolic diffusion of the biosensor, the real ZAP-70 activity within the synapse should be even stronger. In a previous study, Randriamampita et al. observed ZAP-70 activation in both the synapse and the distal pole of synapse (termed “anti-synapse” by the authors) using a membrane-anchored biosensor with a LAT derived sequence.[29] However, we did not observe ZAP-70 activation by Raji B cells in “anti-synapse” using our biosensor or in further confirmation using anti-phospho-ZAP-70 staining (Fig. S5), which is consistent with the previous findings of the receptor-proximal signaling of ZAP-70.

There have been increasing studies suggesting membrane organization as a key player in TCR signaling.[13,17] The early signal transduction initiated by TCR triggering relies heavily on the local balance of kinase and phosphatase activities, which can be spatially regulated by the recruitment of signaling molecules to or their segregation from TCR-CD3 and receptor-proximal signaling complex.[10,24] As a key component of microdomains, cholesterol is found to contribute to normal TCR signaling by regulating TCR-induced phosphorylation. Cholesterol oxidation in 3A9 T hybridoma cells inhibits TCR-induced tyrosine phosphorylation of CD3ζ, ZAP-70 and LAT[11]. Modifications of cholesterol even reduce the binding affinity between pMHC and TCR or CD8.[18,19,22,25] In our study, we visualized altered ZAP-70 activities after cholesterol depletion. MβCD-treated E6.1 cells failed to elicit strong and sustained ZAP-70 activation in response to anti-CD3, or to reduce basal ZAP-70 activity after inhibiting upstream Src family kinase with PP2. This is consistent with previous reports that both basal and TCR-induced phosphorylation of Lck Y394 and ZAP-70 Y319 are greatly reduced by MβCD treatment in peripheral blood T blasts.[30] This impaired signaling dynamics provides further evidence for the essential role of membrane organization in regulating TCR signal transduction.

In our experiments, we noted that photobleaching could distort the current ratiometric representation of FRET changes. Since the default conformation of the ZAP-70 biosensor has a relatively high FRET level, exciting the donor results in faster photobleaching of the acceptor than donor. This translates into a gradual increase of the ECFP/FRET ratio regardless of ZAP-70 activation (Fig. S6a). Photobleaching can also reduce the sensitivity of detection in long time-lapse imaging, as photobleached species (donor, acceptor, or both) may still serve as substrate for ZAP-70, but would be less responsive for FRET changes. Since photobleaching and redistribution of different biosensor species are reaction and diffusion processes, the extent of photobleaching-induced ECFP/FRET ratio increase depends on the amount of photobleached biosensor species during each excitation period, and the duration between consecutive imaging frames for diffusion to disperse in-focus photobleached species. Accordingly, we observed a slower rate of increase in ECFP/FRET

ratio when the frame interval was increased (Fig. S6a & b), with 5-min interval generating almost no photobleaching artifact. Comparing to the 30-sec interval, the 5-sec interval yielded a doubled rate of ratio increase per frame (Fig. S6c), suggesting that 5 sec is not enough for diffusion to equilibrate photobleached biosensor molecules. This is consistent with the relatively slow cytosolic diffusivity (0.93±0.06 μm^2/sec) of the Src biosensor, which has a similar design as the present ZAP-70 biosensor.[26] When photobleaching artifact was minimized with a 5-min frame interval, we restored the kinetics of ZAP-70 activity in response to anti-CD3 stimulation (Fig. S6d). Different from the sustained high ratios under a 30sec-sampling interval, it started to decrease after 5 minutes.

In conclusion, we demonstrated the power of a FRET-based biosensor to report the spatiotemporal activities of ZAP-70 in living cells with subcellular resolution, which provides a unique tool for the analysis of ZAP-70-mediated immunoreceptor signaling.

Supplementary Material

Refer to Web version on PubMed Central for supplementary material.

Acknowledgments

This work was supported by NIH grant R01AI124680 (to C.Z.), NIH HL098472, HL109142, HL121365 (Y.W.). We thank Dr. Arthur Weiss for kindly sharing the Jurkat P116 cell line expressing kinase-inactive ZAP-70.

References

1. Acuto O, Di Bartolo V, Michel F. Tailoring T-cell receptor signals by proximal negative feedback mechanisms. Nat Rev Immunol. 2008; 8:699–712. [PubMed: 18728635]
2. Au-Yeung BB, Deindl S, Hsu LY, Palacios EH, Levin SE, Kuriyan J, Weiss A. The structure, regulation, and function of ZAP-70. Immunol Rev. 2009; 228:41–57. [PubMed: 19290920]
3. Au-Yeung BB, Levin SE, Zhang C, Hsu LY, Cheng DA, Killeen N, Shokat KM, Weiss A. A genetically selective inhibitor demonstrates a function for the kinase Zap70 in regulatory T cells independent of its catalytic activity. Nat Immunol. 2010; 11:1085–1092. [PubMed: 21037577]
4. Bi K, Tanaka Y, Coudronniere N, Sugie K, Hong S, van Stipdonk MJ, Altman A. Antigen-induced translocation of PKC-theta to membrane rafts is required for T cell activation. Nat Immunol. 2001; 2:556–563. [PubMed: 11376344]
5. Boerth NJ, Sadler JJ, Bauer DE, Clements JL, Gheith SM, Koretzky GA. Recruitment of SLP-76 to the membrane and glycolipid-enriched membrane microdomains replaces the requirement for linker for activation of T cells in T cell receptor signaling. J Exp Med. 2000; 192:1047–1058. [PubMed: 11015445]
6. Brdicka T, Kadlecek TA, Roose JP, Pastuszak AW, Weiss A. Intramolecular regulatory switch in ZAP-70: analogy with receptor tyrosine kinases. Mol Cell Biol. 2005; 25:4924–4933. [PubMed: 15923611]
7. Bunnell SC, Hong DI, Kardon JR, Yamazaki T, McGlade CJ, Barr VA, Samelson LE. T cell receptor ligation induces the formation of dynamically regulated signaling assemblies. J Cell Biol. 2002; 158:1263–1275. [PubMed: 12356870]
8. Cadra S, Gucciardi A, Valignat MP, Theodoly O, Vacaflores A, Houtman JC, Lellouch AC. ROZA-XL, an improved FRET based biosensor with an increased dynamic range for visualizing zeta associated protein 70 kD (ZAP-70) tyrosine kinase activity in live T cells. Biochem Biophys Res Commun. 2015; 459:405–410. [PubMed: 25735979]
9. Chen L, Huynh L, Apgar J, Tang L, Rassenti L, Weiss A, Kipps TJ. ZAP-70 enhances IgM signaling independent of its kinase activity in chronic lymphocytic leukemia. Blood. 2008; 111:2685–2692. [PubMed: 18048647]

10. Davis SJ, van der Merwe PA. The kinetic-segregation model: TCR triggering and beyond. Nat Immunol. 2006; 7:803–809. [PubMed: 16855606]
11. Drevot P, Langlet C, Guo XJ, Bernard AM, Colard O, Chauvin JP, Lasserre R, He HT. TCR signal initiation machinery is pre-assembled and activated in a subset of membrane rafts. EMBO J. 2002; 21:1899–1908. [PubMed: 11953309]
12. Dustin ML. Multiscale analysis of T cell activation: correlating in vitro and in vivo analysis of the immunological synapse. Curr Top Microbiol Immunol. 2009; 334:47–70. [PubMed: 19521681]
13. Dykstra M, Cherukuri A, Sohn HW, Tzeng SJ, Pierce SK. Location is everything: lipid rafts and immune cell signaling. Annu Rev Immunol. 2003; 21:457–481. [PubMed: 12615889]
14. Edelstein A, Amodaj N, Hoover K, Vale R, Stuurman N. Computer control of microscopes using microManager. Curr Protoc Mol Biol Chapter 14: Unit14 20. 2010
15. Fargnoli J, Burkhardt AL, Laverty M, Kut SA, van Oers NS, Weiss A, Bolen JB. Syk mutation in Jurkat E6-derived clones results in lack of p72syk expression. J Biol Chem. 1995; 270:26533–26537. [PubMed: 7592872]
16. Grakoui A, Bromley SK, Sumen C, Davis MM, Shaw AS, Allen PM, Dustin ML. The immunological synapse: a molecular machine controlling T cell activation. Science. 1999; 285:221–227. [PubMed: 10398592]
17. He HT, Marguet D. T-cell antigen receptor triggering and lipid rafts: a matter of space and time scales. Talking Point on the involvement of lipid rafts in T-cell activation. EMBO Rep. 2008; 9:525–530. [PubMed: 18516087]
18. Huang J, Edwards LJ, Evavold BD, Zhu C. Kinetics of MHC-CD8 interaction at the T cell membrane. J Immunol. 2007; 179:7653–7662. [PubMed: 18025211]
19. Huang JV, Zarnitsyna I, Liu B, Edwards LJ, Jiang N, Evavold BD, Zhu C. The kinetics of two-dimensional TCR and pMHC interactions determine T-cell responsiveness. Nature. 2010; 464:932–936. [PubMed: 20357766]
20. Huse M. The T-cell-receptor signaling network. Journal of Cell Science. 2009; 122:1269–1273. [PubMed: 19386893]
21. Huse M, Klein LO, Girvin AT, Faraj JM, Li QJ, Kuhns MS, Davis MM. Spatial and temporal dynamics of T cell receptor signaling with a photoactivatable agonist. Immunity. 2007; 27:76–88. [PubMed: 17629516]
22. Jiang N, Huang J, Edwards LJ, Liu B, Zhang Y, Beal CD, Evavold BD, Zhu C. Two-stage cooperative T cell receptor-peptide major histocompatibility complex-CD8 trimolecular interactions amplify antigen discrimination. Immunity. 2011; 34:13–23. [PubMed: 21256056]
23. Lee KH, Dinner AR, Tu C, Campi G, Raychaudhuri S, Varma R, Sims TN, Burack WR, Wu H, Wang J, Kanagawa O, Markiewicz M, Allen PM, Dustin ML, Chakraborty AK, Shaw AS. The immunological synapse balances T cell receptor signaling and degradation. Science. 2003; 302:1218–1222. [PubMed: 14512504]
24. Lillemeier BF, Mortelmaier MA, Forstner MB, Huppa JB, Groves JT, Davis MM. TCR and Lat are expressed on separate protein islands on T cell membranes and concatenate during activation. Nat Immunol. 2010; 11:90–96. [PubMed: 20010844]
25. Liu B, Chen W, Natarajan K, Li Z, Margulies DH, Zhu C. The cellular environment regulates in situ kinetics of T-cell receptor interaction with peptide major histocompatibility complex. Eur J Immunol. 2015; 45:2099–2110. [PubMed: 25944482]
26. Lu S, Ouyang M, Seong J, Zhang J, Chien S, Wang Y. The spatiotemporal pattern of Src activation at lipid rafts revealed by diffusion-corrected FRET imaging. PLoS Comput Biol. 2008; 4:e1000127. [PubMed: 18711637]
27. Mocsai A, Ruland J, Tybulewicz VL. The SYK tyrosine kinase: a crucial player in diverse biological functions. Nat Rev Immunol. 2010; 10:387–402. [PubMed: 20467426]
28. Peters JD, Furlong MT, Asai DJ, Harrison ML, Geahlen RL. Syk, activated by cross-linking the B-cell antigen receptor, localizes to the cytosol where it interacts with and phosphorylates alpha-tubulin on tyrosine. J Biol Chem. 1996; 271:4755–4762. [PubMed: 8617742]
29. Randriamampita C, Mouchacca P, Malissen B, Marguet D, Trautmann A, Lellouch AC. A novel ZAP-70 dependent FRET based biosensor reveals kinase activity at both the immunological synapse and the antisynapse. PLoS One. 2008; 3:e1521. [PubMed: 18231606]

30. Schade AE, Levine AD. Lipid Raft Heterogeneity in Human Peripheral Blood T Lymphoblasts: A Mechanism for Regulating the Initiation of TCR Signal Transduction. The Journal of Immunology. 2002; 168:2233–2239. [PubMed: 11859110]
31. Seong J, Ouyang M, Kim T, Sun J, Wen PC, Lu S, Zhuo Y, Llewellyn NM, Schlaepfer DD, Guan JL, Chien S, Wang Y. Detection of focal adhesion kinase activation at membrane microdomains by fluorescence resonance energy transfer. Nat Commun. 2011; 2:406. [PubMed: 21792185]
32. Sloan-Lancaster J, Presley J, Ellenberg J, Yamazaki T, Lippincott-Schwartz J, Samelson LE. ZAP-70 association with T cell receptor zeta (TCRzeta): fluorescence imaging of dynamic changes upon cellular stimulation. J Cell Biol. 1998; 143:613–624. [PubMed: 9813084]
33. Sloan-Lancaster J, Zhang W, Presley J, Williams BL, Abraham RT, Lippincott-Schwartz J, Samelson LE. Regulation of ZAP-70 intracellular localization: visualization with the green fluorescent protein. J Exp Med. 1997; 186:1713–1724. [PubMed: 9362531]
34. Ting AY, Kain KH, Klemke RL, Tsien RY. Genetically encoded fluorescent reporters of protein tyrosine kinase activities in living cells. Proc Natl Acad Sci U S A. 2001; 98:15003–15008. [PubMed: 11752449]
35. Tsien RY, Harootunian AT. Practical design criteria for a dynamic ratio imaging system. Cell Calcium. 1990; 11:93–109. [PubMed: 2354507]
36. Wacholtz MC, Lipsky PE. Anti-CD3-stimulated Ca2+ signal in individual human peripheral T cells. Activation correlates with a sustained increase in intracellular Ca2+1. J Immunol. 1993; 150:5338–5349. [PubMed: 8515062]
37. Wang H, Kadlecek TA, Au-Yeung BB, Goodfellow HE, Hsu LY, Freedman TS, Weiss A. ZAP-70: an essential kinase in T-cell signaling. Cold Spring Harb Perspect Biol. 2010; 2:a002279. [PubMed: 20452964]
38. Wang Y, Botvinick EL, Zhao Y, Berns MW, Usami S, Tsien RY, Chien S. Visualizing the mechanical activation of Src. Nature. 2005; 434:1040–1045. [PubMed: 15846350]
39. Weiss A. T cell antigen receptor signal transduction: a tale of tails and cytoplasmic protein-tyrosine kinases. Cell. 1993; 73:209–212. [PubMed: 8477442]
40. Xiang X, Sun J, Wu J, He HT, Wang Y, Zhu C. A FRET-Based Biosensor for Imaging SYK Activities in Living Cells. Cellular and Molecular Bioengineering. 2011; 4:670–677. [PubMed: 25541586]
41. Yokosuka T, Sakata-Sogawa K, Kobayashi W, Hiroshima M, Hashimoto-Tane A, Tokunaga M, Dustin ML, Saito T. Newly generated T cell receptor microclusters initiate and sustain T cell activation by recruitment of Zap70 and SLP-76. Nat Immunol. 2005; 6:1253–1262. [PubMed: 16273097]

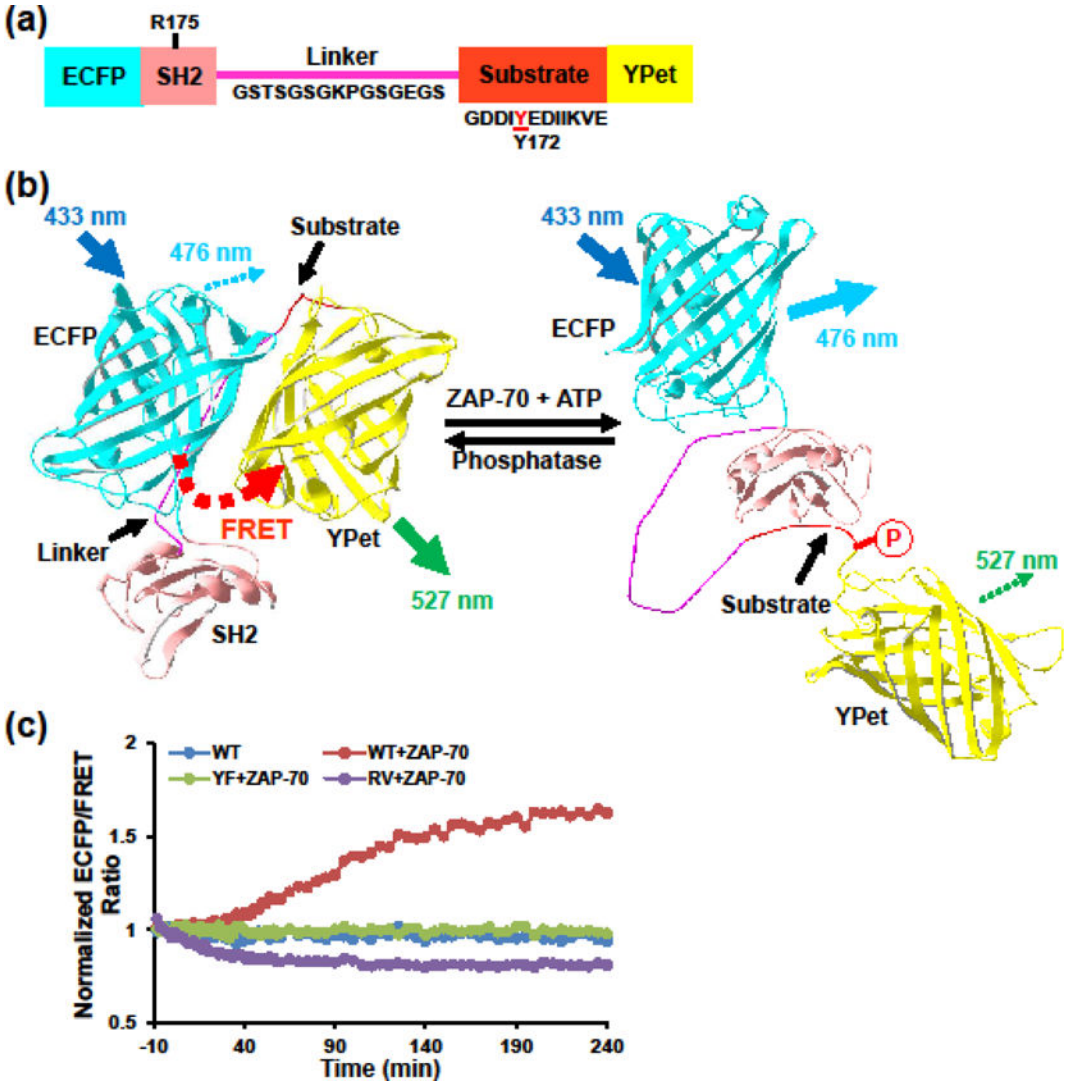

FIGURE 1. Biosensor design and *in vitro* characterization

(a) Biosensor consists of an ECFP domain, an SH2 domain, a flexible linker (sequence indicated), a substrate sequence derived from Vav2 (indicated) containing a tryrosine in position 172, and a YPet domain[40]. **(b)** Schematics showing the mechanism of reporting ZAP-70 activity by FRET changes. Phosphorylation of the substrate peptide induces its intramolecular binding to the SH2 domain, resulting in separation of the ECFP and YPet and thus a decrease in FRET efficiency. **(c)** ECFP/FRET emission ratio (defined as the ratio between emission channels of donor ECFP and acceptor YPet under the same donor excitation) time courses of purified biosensor in response to active ZAP-70 in vitro. Controls included two biosensor mutants with a single residue substitution either at the substrate Tyr172 (YF) or the SH2 R176 (RV).

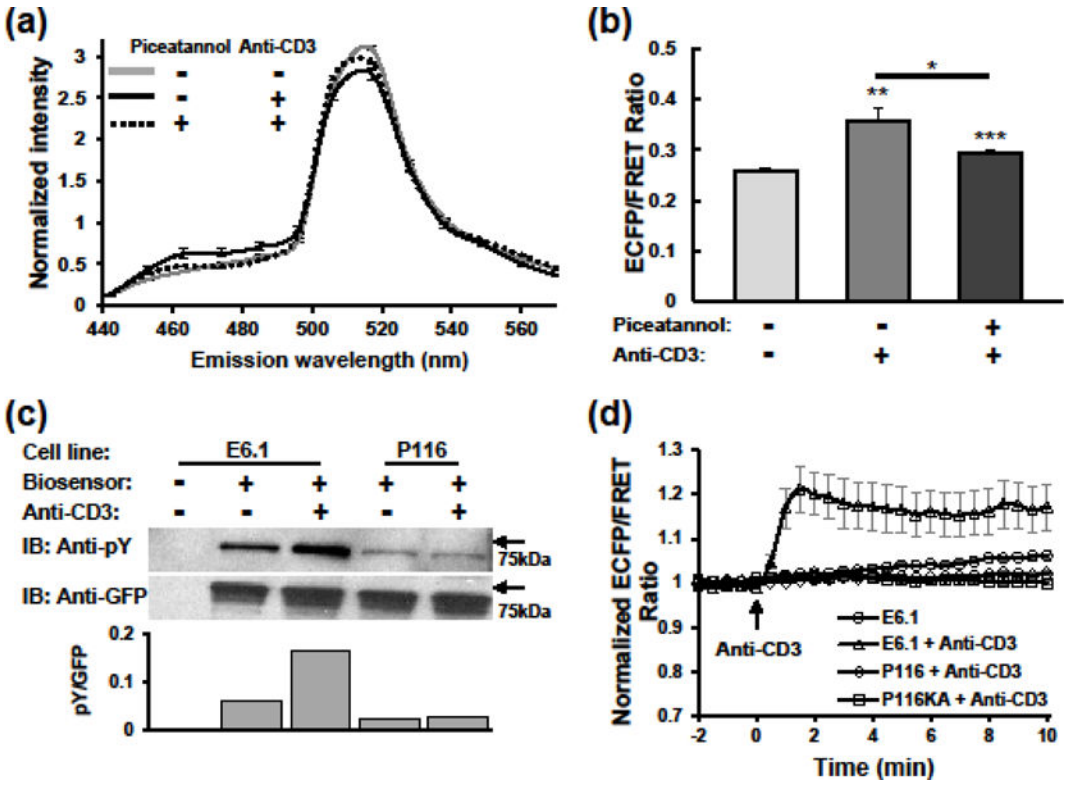

FIGURE 2. ZAP-70-specific biosensor responses in Jurkat T cells

(a) Emission spectra of Jurkat E6.1 cells expressing the biosensor in response to anti-CD3 stimulation. E6.1 cells with or without piceatannol treatment were unstimulated or stimulated with anti-CD3 for 15 min. Spectral images of each cell were acquired using the lambda mode of an LSM510 META confocal microscope. Data represent mean ± SEM from 36, 40, and 73 cells of the three groups from top to bottom, respectively. **(b)** Statistics of 485 nm/517 nm emission ratios calculated from (a). Significance was assessed by Student t-test between the middle and right columns as well as between these two columns and the first one. *, $p<0.05$; **, $p<0.01$; ***, $p<0.001$. **(c)** Western blot analysis of biosensor phosphorylation in Jurkat cells. E6.1 and P116 cells expressing the biosensor were stimulated with anti-CD3 for 10 minutes. Cell lysate were subjected to anti-GFP immunoprecipitation, and analyzed by SDS-PAGE followed by immunoblotting with anti-phosphotyrosine (upper), and stripping and reblotting with anti-GFP (lower). Column plot shows quantification of pY to GFP ratio based on blots intensity. **(d)** Normalized ECFP/FRET ratio time courses of Jurkat E6.1 (n = 9 cells), P116 (n = 23 cells), and P116KA (n = 27 cells) cells expressing the biosensor in response to anti-CD3 (10 μg/ml) stimulation. Control shows background ratio changes in E6.1 cells without stimulation (n = 19 cells). Data represent mean ± SEM of individual cells imaged with Epi-fluorescence microscopy.

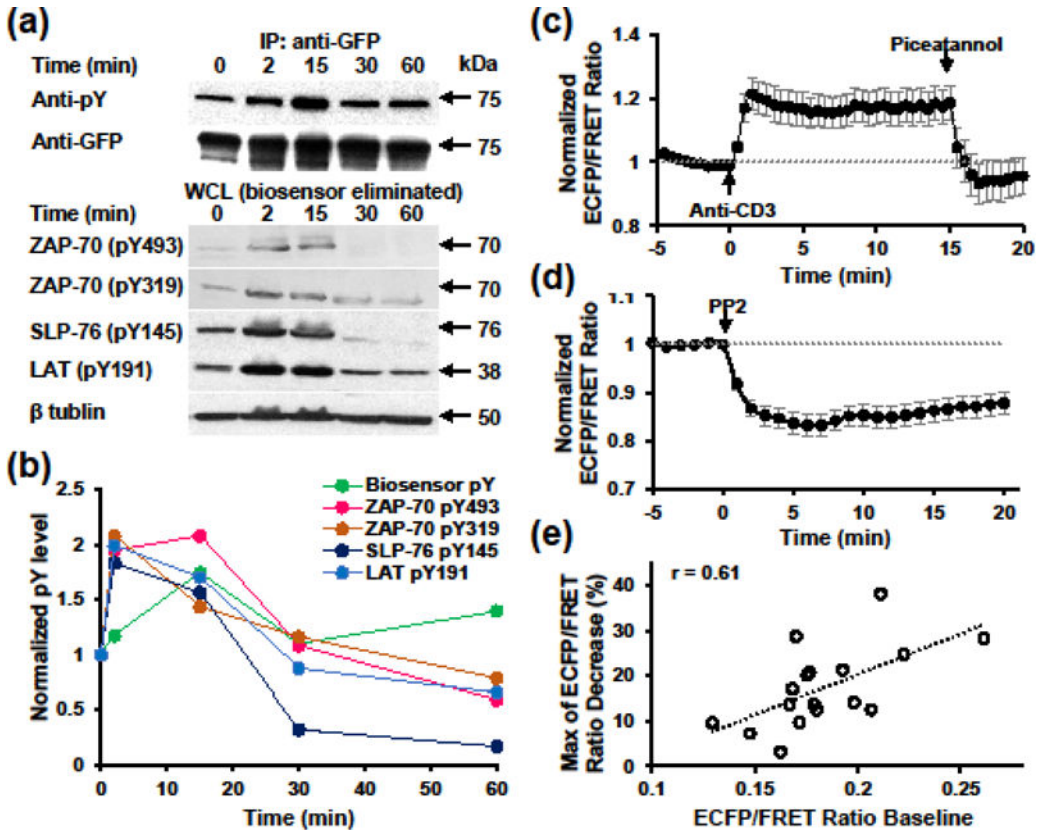

FIGURE 3. Biosensor reports ZAP-70 activities with fast kinetics in Jurkat T cells

(a) Phosphorylation kinetics of the biosensor comparing with endogenous ZAP-70 and its substrate molecules upon stimulation with superantigen-pulsed Raji B cells. Upper, the whole cell lysates were subjected to immunoprecipitation with anti-GFP and subsequent blotting with either anti-pY or anti-GFP. Lower, whole cell lysates post biosensor immunoprecipitation were subjected to western blotting with antibodies indicated. **(b)** Quantification of phosphorylation kinetics using data shown in (a). pY band intensities were normalized by that of loading control and 0 min time point. **(c)–(d)** Normalized ECFP/FRET ratio time course (mean ± SEM) of Jurkat E6.1 cells expressing the biosensor in response to anti-CD3 (10 μg/ml) and subsequent piceatannol (10 μg/ml) stimulation (b, n = 9 cells) or PP2 (10 μM) stimulation (c, n = 17 cells). **(e)** Correlation analysis between ECFP/FRET ratio baseline and the maximum ratio decrease followed by PP2 treatment in (c).

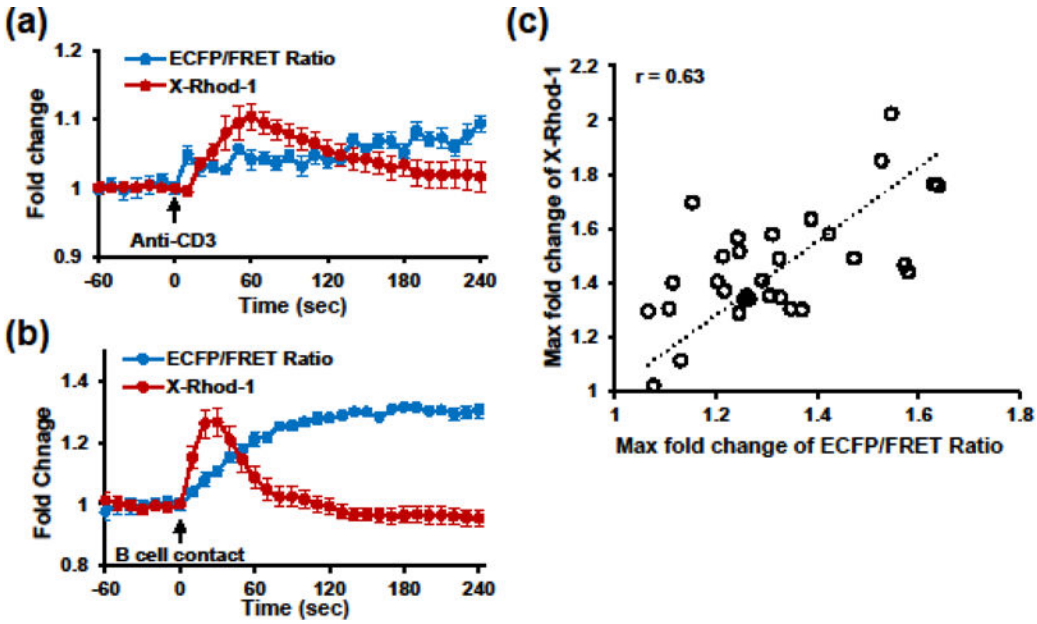

FIGURE 4. Concurrent imaging of ZAP-70 activation and calcium flux upon TCR stimulation

(a)–(b) Time courses (mean ± SEM) of normalized ECFP/FRET ratio for ZAP-70 activity (blue curve) and X-rhod-1 intensity for intracellular calcium flux (red curve) of individual Jurkat E6.1 cells stimulated with 10 μg/ml soluble anti-CD3 (a, n = 19 cells), or superantigen-pulsed Raji B cells (b, n = 37 cells). **(c)** Correlation analysis between maximum fold changes of ECFP/FRET ratio and X-Rhod-1 intensity within 120 sec upon B cell contact.

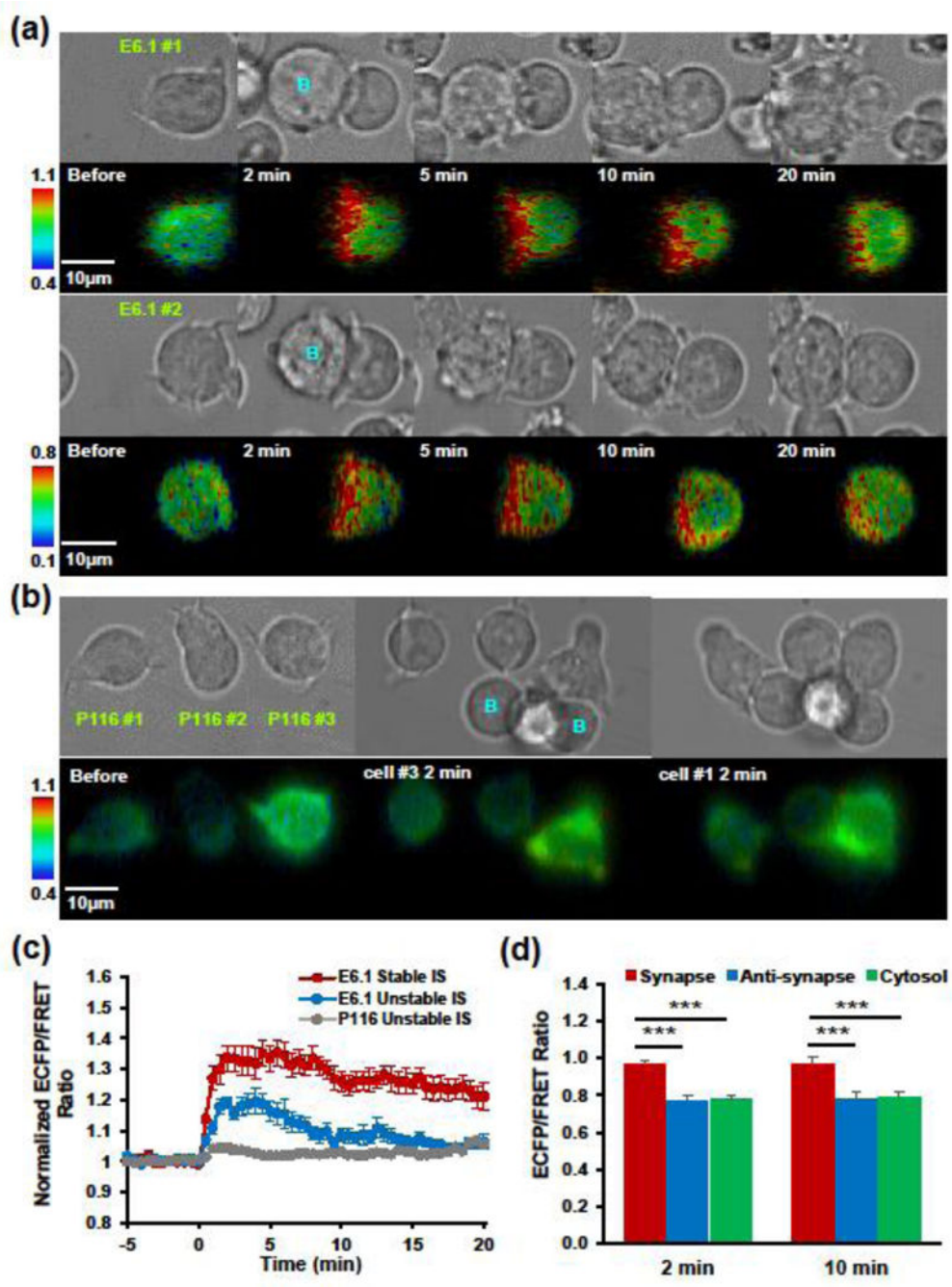

FIGURE 5. Biosensor reveals local ZAP-70 activation within the immunological synapse

(a) Representative image series showing ZAP-70 activation within the immunological synapse formed between Jurkat E6.1 cells (green label, E6.1 #1 and #2) and superantigen-pulsed Raji B cells (blue label, B). Upper, bright field images of synapse formation; lower, ECFP/FRET ratio images in IMD display with the hue component indicating ECFP/FRET ratio and the value component indicating YPet fluorescence. **(b)** Representative image series (Upper, bright field; lower, ECFP/FRET ratio images in IMD display) of Jurkat P116 cells (green label, E6.1 #1 #2, and #3) interacting with superantigen-pulsed Raji B cells (blue

label, B). **(c)** Normalized ECFP/FRET ratio time courses (mean ± SEM) calculated across the whole cell region. Stable immunological synapse (IS) is defined as one lasting for more than 15 min. E6.1 stable IS, n = 10 cells. E6.1 unstable IS, n = 6 cells. P116 unstable IS, n = 9 cells. **(d)** Comparison of ECFP/FRET ratio among different subcellular compartments. Anti-synapse, the opposite pole of synapse.

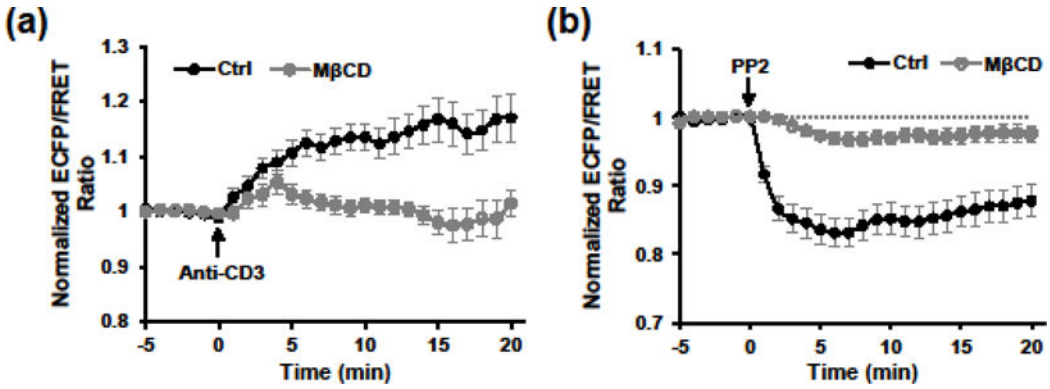

FIGURE 6. MβCD treatment impairs ZAP-70 activities in response to upstream stimuli

(a) Normalized ECFP/FRET ratio time courses of Jurkat E6.1 cells expressing the biosensor in response to anti-CD3 (10 μg/ml) stimulation with (n = 32 cells) or without (n = 26 cells) MβCD pretreatment. **(b)** Normalized ECFP/FRET ratio time courses of Jurkat E6.1 cells expressing the biosensor in response to PP2 (10 μM) stimulation with (n = 18 cells) or without (n = 17 cells) MβCD pretreatment.